ACS APPLIED MATERIALS & INTERFACES

www.acsami.org

Research Article

Comparison of the Mechanical Properties of a Conjugated Polymer Deposited Using Spin Coating, Interfacial Spreading, Solution Shearing, and Spray Coating

Kartik Choudhary,[‖] Alexander X. Chen,[‖] Gregory M. Pitch, Rory Runser, Armando Urbina, Tim J. Dunn, Moses Kodur, Andrew T. Kleinschmidt, Benjamin G. Wang, Jordan A. Bunch, David P. Fenning, Alexander L. Ayzner, and Darren J. Lipomi*

Cite This: https://doi.org/10.1021/acsami.1c13043

Read Online

ACCESS | Metrics & More | Article Recommendations | Supporting Information

ABSTRACT: The mechanical properties of π-conjugated (semiconducting) polymers are a key determinant of the stability and manufacturability of devices envisioned for applications in energy and healthcare. These properties—including modulus, extensibility, toughness, and strength—are influenced by the morphology of the solid film, which depends on the method of processing. To date, the majority of work done on the mechanical properties of semiconducting polymers has been performed on films deposited by spin coating, a process not amenable to the manufacturing of large-area films. Here, we compare the mechanical properties of thin films of regioregular poly(3-heptylthiophene) (P3HpT) produced by three scalable deposition processes—interfacial spreading, solution shearing, and spray coating—and spin coating (as a reference). Our results lead to four principal conclusions. (1) Spray-coated films have poor mechanical robustness due to defects and inhomogeneous thickness. (2) Sheared films show the highest modulus, strength, and toughness, likely resulting from a decrease in free volume. (3) Interfacially spread films show a lower modulus but greater fracture strain than spin-coated films. (4) The trends observed in the tensile behavior of films cast using different deposition processes held true for both P3HpT and poly(3-butylthiophene) (P3BT), an analogue with a higher glass transition temperature. Grazing incidence X-ray diffraction and ultraviolet−visible spectroscopy reveal many notable differences in the solid structures of P3HpT films generated by all four processes. While these morphological differences provide possible explanations for differences in the electronic properties (hole mobility), we find that the mechanical properties of the film are dominated by the free volume and surface topography. In field-effect transistors, spread films had mobilities more than 1 magnitude greater than any other films, likely due to a relatively high proportion of edge-on texturing and long coherence length in the crystalline domains. Overall, spread films offer the best combination of deformability and charge-transport properties.

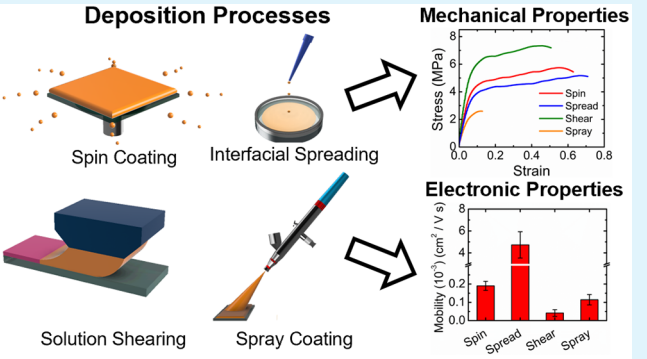

KEYWORDS: *mechanical properties, semiconducting polymers, roll-to-roll deposition, morphology, polymers*

1. INTRODUCTION

Semiconducting (π-conjugated) polymers are amenable to the manufacturing of devices covering large areas in part because of their ability to be deposited from solution; that is, polymer-based solar cells, solid-state lighting, wearable sensors, display technologies, and other devices have the potential to be manufactured using processes analogous to ink-based printing.[1−3] One requirement central to all envisioned applications of devices intended for use in these flexible form factors is mechanical robustness. The mechanical properties of a polymer are dependent not only on its molecular structure but also on its morphology. The morphology in the solid state is the result of an interplay of processes, which include the kinetics of solidification and the forces present during deposition.[4] However, the majority of mechanical data for conjugated polymer films have been obtained from films prepared by spin coating,[5−7] which is not amenable to large-area deposition or deposition on flexible substrates.[8] It is not clear how the mechanical properties are influenced by processes of deposition that have the potential for scalability, such as interfacial spreading, solution shearing, and spray

Received: July 10, 2021
Accepted: October 8, 2021

coating (Figure 1). The purpose of this work is to elucidate how the mechanical properties of a conjugated polymer film—as mediated by its morphology—are influenced by different deposition processes.

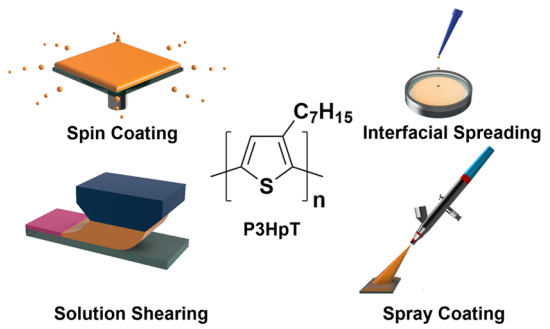

Figure 1. Films of P3HpT were cast using four different deposition processes: spin coating, interfacial spreading, solution shearing, and spray coating.

2. BACKGROUND

The manner in which a material is processed is crucial to its physical properties in an engineering application. For polymeric materials, the processing conditions influence the crystallinity, density, glass transition temperature, extent of entanglement, topography, texture, and defects.[9] For semiconducting polymers, these characteristics determine not only the mechanical response but also the electronic properties.[10−12] Most studies on the mechanical properties of conjugated polymers use molecular characteristics as the independent variables in experiments;[13−15] that is, parameters such as side chain length, molecular weight, or single atoms in the backbone are altered systematically. In most of these studies, with few exceptions,[16−18] the films are deposited using spin coating, which cannot be readily scaled.

Nevertheless, among the first to study the role of solution processing on the mechanical properties of semiconducting polymers was the O'Connor group, who modified the speed and concentration during spin coating to manipulate the kinetics of solidification of bulk heterojunction films of poly(3-hexylthiophene) and [6,6]-phenyl-C_{61}-butyric methyl ester (P3HT:$PC_{61}BM$).[4] Films spun at lower speeds had greater short-range order in photophysical aggregates (as determined by the weakly interacting H-aggregate model).[19] Films with greater order had higher elastic moduli (i.e., increased stiffness) but lower fracture strains (i.e., extensibility). In molecular dynamics simulations performed in our laboratory, Root et al. found that processes designed to mimic solidification from the melt phase had a larger density of entanglements and an increased modulus compared to those modeled to be solidified from solution in a poor solvent.[20] However, such simulations are currently unable to predict the formation of crystallites and micron-scale defects, which are of critical importance to the mechanical properties of the solid film.

This work seeks to elucidate how scalable, roll-to-roll compatible deposition processes affect the morphology and mechanical properties of a polymer film. To guarantee a wide range of morphologies—and thus mechanical properties—we explored four solution-phase deposition processes which rely on different processing conditions: spin coating, interfacial spreading, solution shearing, and spray coating. Unlike spin coating, the other three processes (spreading, shearing, and spraying) have the potential to be used in continuous forms of deposition, that is, roll-to-roll manufacturing.[21]

3. EXPERIMENTAL DESIGN

3.1. Choice of Deposition Processes. We chose three deposition processes which have the potential for scalability—interfacial spreading (i.e., "floating film-transfer method"), solution shearing (i.e., "blade coating"), and spray coating—and compared the mechanical properties to films produced by spin coating. Interfacial spreading ("floating film-transfer method") is a process in which a polymer solution is drop-cast on the surface of a liquid with a high surface tension, typically water.[22] The process relies on Marangoni spreading and results in solidification upon evaporation of the solvent.[23,24] The resulting films are air-stable once solidified and can then be transferred (e.g., "stamped") directly from the water bath to planar or textured substrates.[25−27] Interfacial spreading also allows for sequential film deposition from orthogonal solvents by stamping coatings layer by layer.[28,29]

Solution shearing is a process by which a blade, attached to a linear actuator, is used to coat solution over a substrate. Shearing has been shown to induce the alignment of polymer backbones[30,31] and influence the lattice spacing in the solid film.[32,33] The shearing process resembles that of slot-die coating, a process common in industrial manufacturing of inks and polymeric thin films.[8]

Finally, spray coating uses an airbrush to deposit films on a surface, which enables two-dimensional patterning of the solid film using shadow masks. Spray-coated films are characterized by their granular topography, which is due to the pressurized atomization of solution droplets.[34,35] Previous studies have shown that spray-coated films are more disordered than their spin-coated counterparts, yet are able to retain the same hole mobilities in thin-film transistors and power-conversion efficiencies in solar cells.[36−38]

3.2. Choice of Polymer and Solvent. As a test material, we chose regioregular poly(3-heptylthiophene) (P3HpT). Compared to its more widely used analogue, P3HT, P3HpT has a lower glass-transition temperature (T_g) and greater deformability.[39] Chlorobenzene was used as the solvent due to the favorable spreading parameter on water (for interfacial spreading) and ability to solubilize P3HpT without clogging the airbrush used in spray coating.[23,24] Because the glass transition temperature of P3HpT is below room temperature, we did not explore the effects of thermal annealing. However, previous studies have suggested that annealing has a significant impact on the morphology and mechanical properties.[40,41]

3.3. Mechanical Testing. Stress−strain measurements of thin films were obtained using a pseudo-freestanding tensile test, that is, "film-on-water".[42] In this method, the ends of the dogbone-shaped film are adhered to polydimethylsiloxane (PDMS) slabs on a linear actuator by van der Waals forces, and the load of the polymer film is measured as it is elongated.

3.4. Morphological Characterization. Optical microscopy was used to investigate the global uniformity of the film, and atomic force microscopy (AFM) was used to investigate the nanoscale surface structure. Aggregation in conjugated polymers provides short-range order and has the potential to contribute to interchain charge transport in conjugated polymers.[43] Here, aggregate fraction was determined using ultraviolet−visible spectroscopy (UV−vis). UV−vis was also used to measure the dichroic ratio of sheared films. Grazing incidence X-ray diffraction (GIXD) measurements were performed to measure the atomic spacing, anisotropy of the domains, relative degree of crystallinity (rDoC), coherence length, and texture of the crystallites (i.e., edge-on vs face-on).

3.5. Thermal Characterization. To investigate how the deposition processes affect the glass transition temperature of the deposited thin film, we used a technique previously developed by our research group in which the UV−vis spectrum of a film is incrementally scanned at increasing temperatures until a change in the spectrum is measured.[44] These measurements would be difficult

https://doi.org/10.1021/acsami.1c13043
ACS Appl. Mater. Interfaces XXXX, XXX, XXX−XXX

to perform for P3HpT because its glass transition temperature is below room temperature.[39,44] Thus, we chose to use poly(3-butylthiophene) (P3BT), which has a higher glass transition temperature (~65 °C, due to the shorter alkyl chain length),[45] as a proxy.

3.6. Electronic Characterization. To understand how morphological changes induced by different deposition processes affect the electronic performance, we obtained measurements of hole mobility from bottom-gate bottom-contact transistors. The electrode material for the source and drain contact was gold. The substrates were modified with an octadecyltrichlorosilane surface treatment, which has been shown to enhance the growth of crystallites on the substrate.[46] In addition, the polymer films were annealed at 100 °C for 1 h in a nitrogen-filled glovebox in order to remove any residual solvent trapped in the film and to improve the morphology of the film.[40] Previous work has shown that stamping an interfacially spread film from above (e.g., from the polymer−air interface) or below (e.g., from the polymer−water interface) influences the mobility of the resulting OFET device.[23] Semiconducting polymer films have been shown to have better mobilities in OFET devices when the transport layer is formed at the polymer−air interface.[23,47] For this reason, we chose to fabricate our interfacially spread OFET devices by stamping the P3HpT film from the polymer−air interface.

4. RESULTS AND DISCUSSION

4.1. Optical Microscopy. Films produced by spin coating (Figure 2a) and shearing (Figure 2c) were uniform at the scale

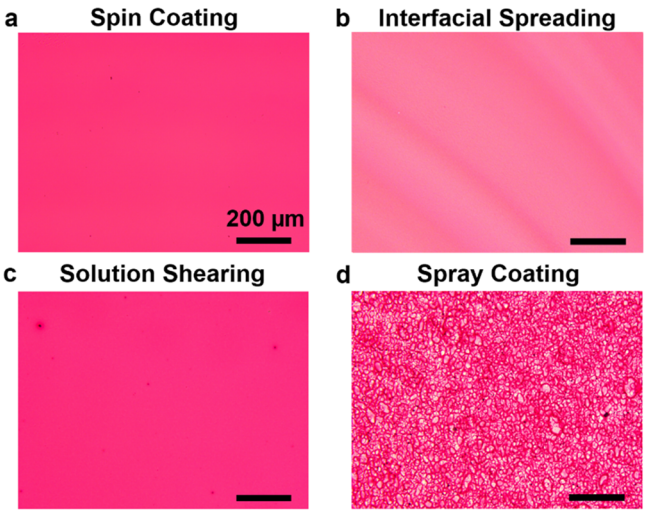

Figure 2. Optical microscopy images of (a) spin-coated, (b) interfacially spread, (c) sheared, and (d) spray-coated films. Spray-coated films have a granular topography, while spread films have regions of lamellar zones of uneven thicknesses.

observable by optical microscopy. This finding is in contrast to interfacial spreading (Figure 2b) and spray coating (Figure 2d), which produced inhomogeneous films. Spread films showed alternating light and dark bands, corresponding to thinner and thicker regions (Video S2).[26,27] Spray coating results in a granular surface (Figure 2d) due to the atomization of solution from the airbrush.[34,35]

4.2. Mechanical Properties of Films Obtained Using Different Deposition Processes. The mechanical response of the films produced by the four different deposition processes is shown in Figure 3. The most prominent features of the data are (1) the low apparent strength and modulus, and high brittleness, of the spray-coated films, (2) the high extensibilities (and overall similar mechanical response) of the spin-coated and spread films, and (3) the high modulus and strength of the sheared films. The mechanical behavior of spray-coated films appeared to be dominated by the accumulation of stress around inhomogeneities that serve as point defects that concentrate stress (Figure S1). Spin-coated and spread films displayed similar mechanical responses. The slightly lower modulus of spread films is possibly due to their inhomogeneous thickness (which in turn could possibly be a consequence of the relatively high concentration of polymer solution) or the influence of the aqueous substrate during the film formation process (Figure 2b). (The average and standard deviation of the thickness for each sample was measured using UV−vis, as shown in Figure S2.) The lower modulus and higher fracture strain of spread films relative to spin-coated films are consistent with the results of an earlier study by our laboratory,[26] as well as previous studies elucidating effects of thickness on the mechanical properties of ultrathin polymer films.[6,48] Finally, sheared films had the greatest modulus, tensile strength, and toughness, despite the topographies of sheared films being indistinguishable from those of spin-coated films (Figure 2).

The directionality of the shearing process suggested that chain alignment might play a role in the increased modulus and strength of sheared films.[49] Ultimately, AFM images, dichroic ratio measurements, and GIXD line plots along the parallel and perpendicular axes all suggest that shearing did not produce observable anisotropy (Figure S3). Likewise, although previous studies have suggested that interfacial spreading can produce anisotropic films,[50,51] our dichroic measurements of spread P3HpT films do not show evidence of anisotropy (Figure S4). While spread and sheared films can show chain alignment (i.e., anisotropy), producing anisotropic films often requires optimization of the processing parameters (e.g., solvent, concentration, deposition rate, or annealing temperature).[50] For example, in sheared films, the degree of anisotropy can be a function of shear speed and annealing temperature.[30,32]

4.3. Effect of the Deposition Process on the Glass Transition Temperature. We examined other characteristics associated with mechanical robustness in order to elucidate (1) the high modulus, strength, and toughness of sheared films and (2) the high extensibility of interfacially spread films. A film with high strength and modulus generally has a high glass transition temperature (T_g) as a result of greater packing density and decreased free volume between polymer chains in amorphous domains.[6,7] Therefore, we hypothesized that the differences in the mechanical behavior between spin-coated and sheared films could be due to the deposition process affecting the packing density (i.e., free volume, and therefore also the glass transition temperature). Likewise, we reasoned that films with greater fracture strains likely also have a greater number of entanglements between polymer chains,[6] which possibly also affects the density. The key role of T_g in predicting the thermomechanical properties of poly(3-alkylthiophenes) is well known.[6,14,39,45] To test our hypothesis, we used UV−vis spectroscopy to compare the glass transition temperature of films produced using shearing, spreading, and spin coating (Figures 4 and S5).[44] However, the low T_g of P3HpT (approximately −12 °C)[45] would make this experiment difficult, as the film would have to be cast at a temperature below the glass transition temperature. For this reason, we performed our thermal and mechanical measurements on P3BT (Figure 4). The purpose of using P3BT as

https://doi.org/10.1021/acsami.1c13043
ACS Appl. Mater. Interfaces XXXX, XXX, XXX−XXX

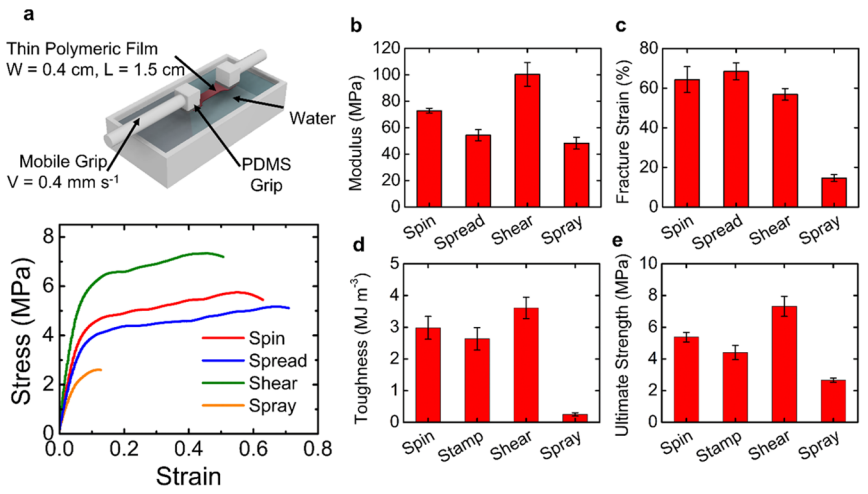

Figure 3. Mechanical properties of P3HpT films (120 nm) measured using the film-on-water tensile testing technique. (a) Top: schematic of the tensile testing setup. Bottom: representative stress−strain curves of P3HpT films cast using different deposition processes. Mechanical properties extracted from the stress−strain curves are (b) fracture strain, (c) elastic modulus, (d) toughness, and (e) ultimate tensile strength. Standard deviations are calculated from a minimum of four stress−strain measurements per deposition process.

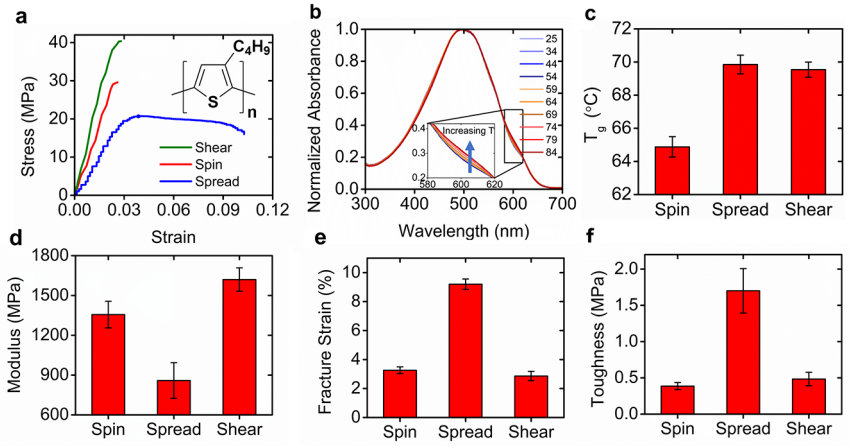

Figure 4. Mechanical and thermal properties of P3BT films cast using spin coating, interfacial spreading, and solution shearing. (a) Stress−strain curves show that sheared films had a greater modulus and tensile strength than those produced using spin coating, while spread films had greater fracture strains. The chemical structure of P3BT is shown in the inset. (b) Progression of absorption spectra for a reference P3BT film relative to the annealing temperature. Inset shows the progression of aggregation as the annealing temperature is increased. The sample spectra shown above are of a spin-coated film of P3BT. (c) The glass transition temperatures of both sheared and spread films were approximately 5 °C greater than their spin-coated counterparts. The (d) modulus, (e) fracture strain, and (f) toughness are extracted from the stress−strain curves.

opposed to P3HpT is twofold. First, P3BT has a shorter alkyl chain length and thus a glass transition temperature above room temperature (Figure 4).[45] Second, we use P3BT as a model polymer in order to elucidate whether the mechanical effects we observe with P3HpT are reproducible with a higher-T_g polymer.

When comparing spin coating, interfacial spreading, and solution shearing, the mechanical response of P3BT mirrors that obtained for P3HpT; that is, sheared films, again, show higher modulus, strength, and toughness than their spin-coated counterparts (Figure 4a,d). Likewise, spread films again show a lower modulus and higher fracture strain (Figure 4a,d,e). Encouragingly, this finding suggests that the effect of the deposition process on the tensile response is consistent for both higher-T_g and lower-T_g P3ATs. We note that the thickness of spread P3BT films (~80 nm) differed greatly from their spun (~110 nm) and sheared (~110 nm) counterparts (Figure S6). This difference is attributed to the difficulty of spreading uniform P3BT films of comparable thicknesses without inhomogeneities or wrinkles (Figure S7).

From the temperature that corresponds to the onset of aggregation by UV−vis spectroscopy (Figures 4b, S5), we see that the T_g of sheared and spread films were approximately 5 °C higher than that of spin-coated films (Figure 4c). Increased T_g is associated with a reduction in free volume, an increase in van der Waals forces and a concomitant increase in cohesive energy density, and possibly also an increase in the density of entanglements.[6,15,45] Based on these findings for P3BT, it is likely that similar morphological differences (i.e., decreased free volume) account for the increased elastic modulus and tensile strength for sheared P3HpT films (Figure 3b,e).

Interestingly, spread P3BT films showed a higher T_g despite having a lower modulus than spin-coated films. This suggests to us that the film formation process on an aqueous substrate affects the amorphous morphology of the film, which in turn is a cause of the greater fracture strains. Notably, spread P3BT

https://doi.org/10.1021/acsami.1c13043
ACS Appl. Mater. Interfaces XXXX, XXX, XXX−XXX

films showed fracture strains approximately 3 times that of spun and sheared films (Figure 4e), resulting in films with the greatest toughness (Figure 4f). Therefore, we see that solution shearing and interfacial spreading both result in a significant difference in the amorphous morphology relative to spin-coated films and that their decreased free volumes manifest in their respective tensile responses in two different ways: a high strength and modulus for sheared films and a high fracture strain for spread films, both of which are able to improve the toughness of the film.

4.4. Effect of Aggregation and Time of Solidification. Previous work from our group has suggested that slower solidification may be correlated with a decrease in free volume within the polymer film, which corresponds with an increase in the modulus.[20,26] This finding is consistent with our comparison of spun and sheared films, in which we show that sheared films have the lowest free volume and slowest solidification rate (Figures 4c, 5a), which then corresponds to the highest modulus (Figure 3b). Studies have also pointed to a correlation of aggregation behavior on the mechanical properties of conjugated polymers, with higher aggregate fraction corresponding to films with a higher elastic moduli.[4,39] We determined the fraction of aggregation in P3HpT and P3BT films using the weakly interacting H-aggregate model developed by Spano and co-workers (Figure 5a).[19] This model approximates the aggregates of P3ATs in a solid film as weakly interacting H-aggregates by comparing the relative peak intensities of the 0−0 and 0−1 vibronic transitions.[19] These vibronic transitions are represented as Gaussian distributions fitted to the measured aggregate absorption of the deconvoluted spectra.[19] The correlation between the aggregate fraction and mechanical properties was weak: the aggregate fraction of all P3HpT films was similar (~0.55), with the exception of those that were spray-coated (Figure 5a). Interestingly, the process with the fastest solidification, spray coating, also had the highest fraction of aggregation. The similarity in aggregate fraction of the spun, sheared, and spread P3HpT films—which nevertheless have disparate mechanical behavior—suggests that other morphological features are responsible for differentiating the mechanical response.

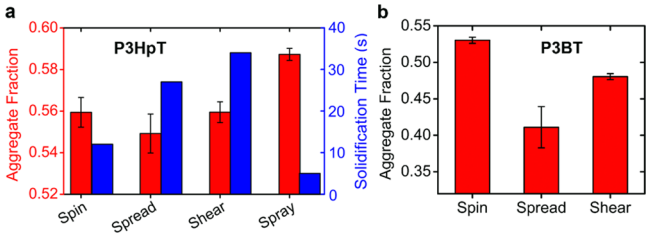

Figure 5. (a) Solidification time (blue) and aggregate fraction (red) relative to the deposition process used for P3HpT films. Solidification time was qualitatively determined as the time necessary for >90% of the P3HpT solution (bright orange) to form a film (dark red) after deposition. (b) Aggregate fraction of P3BT films.

Work from the O'Connor group has suggested that faster film formation (i.e., faster spin speeds) results in films with lower aggregate fractions.[4] However, we see no significant differences in aggregate fraction between spun, spread, and sheared films despite differing solidification times. The similarity in the aggregation behavior itself may be a consequence of the low T_g of P3HpT (−12 °C).[39] The positioning of this second-order phase transition below room temperature may allow for some degree of equilibration between aggregated and nonaggregated domains during film formation. Our hypothesis is validated by a comparison of aggregate fraction in P3BT films (Figure 5b), which show the same trends between spun, spread, and sheared films, yet with a far greater correlation (i.e., quantifiable differences in aggregation). For example, a difference of ~0.02 between the aggregate fractions of spun and spread P3HpT films compared to a difference of ~0.13 between P3BT films prepared using the same two methods. Likewise, a comparison of the aggregate fractions of spun and spread films suggest that the low aggregation of spread films could possibly contribute to their low modulus and tensile strength. That is to say, the relative difference between both the aggregation and the modulus of spun films and sheared films is much greater for P3BT (Figures 5b and 4d) than for P3HpT (Figures 5b and 3b).

4.5. Correlation of Mechanical and Structural Data with Charge-Transport Properties. In some types of conjugated polymer (e.g., polythiophenes), charge transport and mechanical deformability have been found to be antithetical.[52,53] Recently, however, numerous studies have shown that synthetic approaches to obtaining favorable charge transport and mechanical deformability can be successful.[54,55] To determine the effect of the deposition process on the transport properties of P3HpT—as mediated by the morphology of the resulting film—we fabricated bottom-gate, bottom-contact field-effect transistors (OFETs, Figure 6).

Spin-coated, spray-coated, and sheared films all had hole mobilities near 0.1×10^{-3} cm^2 V^{-1} s^{-1} (Figure 6b, with output and transfer characteristics shown in Figure 6c−f and mobility extractions from all device measurements found in Figure S8). Sheared films showed the lowest mobilities among the four deposition processes. Spray-coated films had mobilities comparable to spin-coated films, which is consistent with previous results reported in the literature.[36−38] However, the most notable observation is that films formed by interfacial spreading demonstrated the highest hole mobilities by over 1 magnitude (Figure 6b). The high mobility of spread films relative to their spin-coated counterparts has been observed previously.[22,47,51] This increase in mobility has been attributed to increased edge-on texturing in spread films,[22,28,51,56] as well as an increase in crystallinity.[27,51]

4.6. Influence of Crystalline Features on the Mechanical and Electronic Properties of P3HpT Films. To elucidate the effect of crystalline features in P3HpT films on the mechanical and electronic properties, we performed GIXD measurements (Figure 7). Spin-coated, spread, and sheared films showed similar Bragg reflections with three distinct lamellar peaks along the Q_z axis (100, 200, and 300) and a π-stacking peak (010) along the Q_{xy} axis (near 1.6 Å^{-1}). Spray-coated films showed much weaker intensities of higher-order lamellar reflections [the (200) and (300) peaks], as is evident from 2D-images (Figure 7a) and the orientationally averaged $I-Q$ plot (Figure 7e). While all four films had similar π-stacking distances, there were more observable differences in lamellar packing distances (Figure 7b). Such a result is not surprising, considering that $\pi-\pi$ interactions are stronger than the relatively weaker van der Waals forces between the aliphatic side chains of the polymer that govern lamellar spacing.[65−67]

Additionally, it is possible that differences in crystallite orientation—i.e., texture—with respect to the film geometry

https://doi.org/10.1021/acsami.1c13043
ACS Appl. Mater. Interfaces XXXX, XXX, XXX−XXX

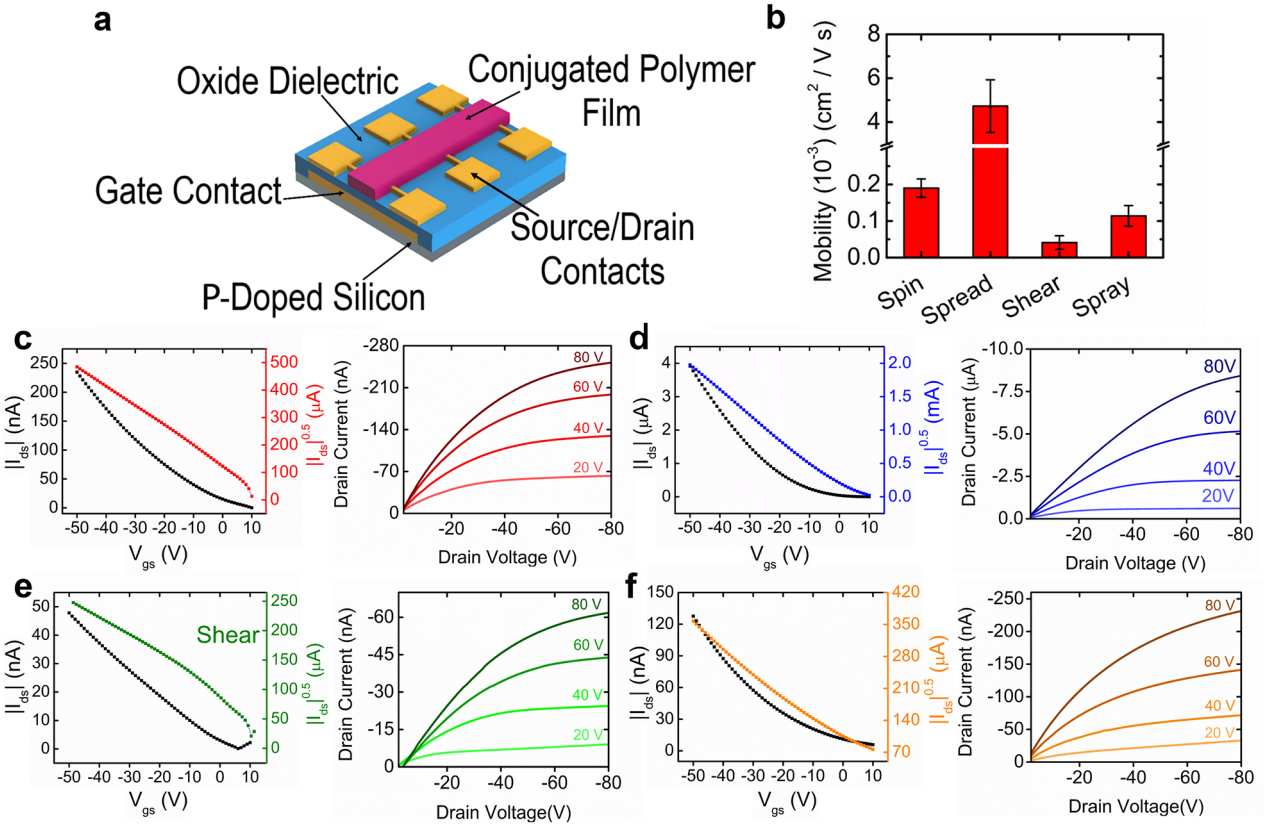

Figure 6. Charge-transport properties of P3HpT films. (a) Schematic of bottom-gate, bottom-contact transistors used to measure the mobility of P3HpT films cast from different deposition techniques. (b) Deposition process showing a significant effect on the mobility of the device as shown by the transfer (left) and output (right) characteristics across (c) spin-coated, (d) spread, (e) sheared, and (f) spray-coated films.

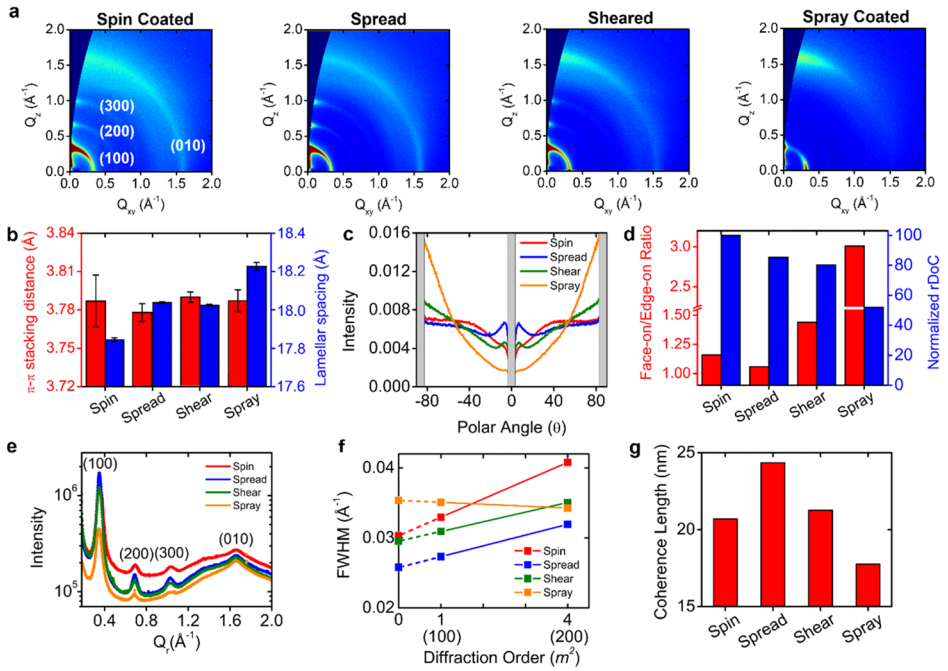

Figure 7. GIXD was used to obtain crystallographic information for P3HpT films cast using different deposition processes. (a) Diffraction images of spin-coated, spread, sheared, and spray-coated films. (b) Variations in $\pi-\pi$ stacking distance and lamellar packing distance across the different films. (c) Crystallite orientation distribution functions (ODF) were obtained from the (100) Bragg peak for each film and used to calculate both the (d) face-on to edge-on population ratio and relative degree of crystallinity (rDoC). (e) Reduced $I(Q_r)$ vs Q_r (where Q_r is the scattering vector length) plots were determined from the diffraction images and used to calculate the (f) full width at half-maximum (fwhm) of the (100) and (200) peaks, which is shown as a function of the square of the diffraction order (m^2). The y-intercept of the fwhm-m^2 relationship was used to calculate the (g) coherence length in the different films.

https://doi.org/10.1021/acsami.1c13043
ACS Appl. Mater. Interfaces XXXX, XXX, XXX−XXX

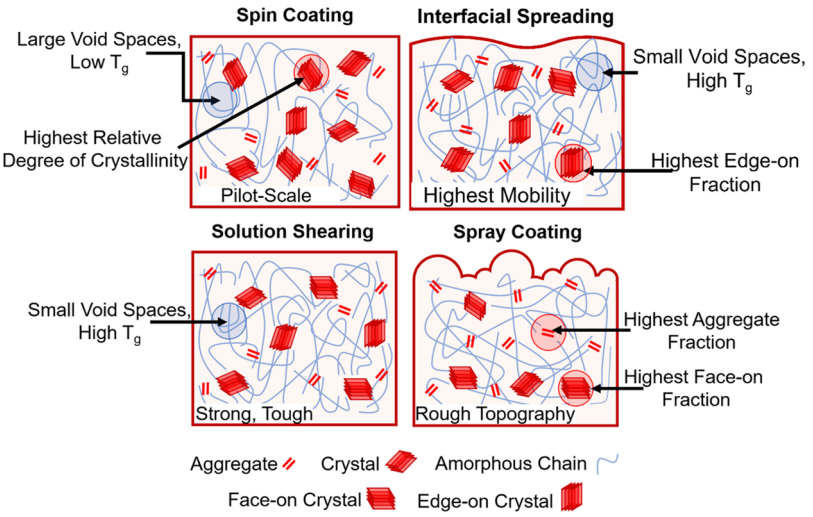

Figure 8. Schematic diagrams highlighting differences in morphology and topography for P3HpT films deposited using the four processes studied in this work. The number of aggregates and crystalline domains are representative of the aggregate fraction and relative degree of crystallinity in these films. The primary features are (1) the topographical differences in spread and spray-coated films, (2) the predominantly face-on texturing of spray coated films, and (3) the high density (low free volume, as depicted by the greater number of chains in the amorphous regions) of sheared and spread films.

and substrate plane have an effect on the mechanical[49] and electronic responses.[57] From the orientation distribution function (ODF) of scattering intensities for the (100) signatures relative to the polar angle (Figure 7c), we are able to quantify the texture exhibited by each film (Figure 7c). Spray-coated films differed from the other three in that they displayed high scattering intensities at higher angles (near ±90°) and low scattering intensities at low angles (~0°), suggesting that spray-coated films preferentially form face-on crystallites (i.e., where the side chain is aligned parallel to the substrate and π-stacking is out-of-plane). In contrast, spin-coated, spread, and sheared films all showed more uniform intensities across all angles (aside from a sharp increase in intensity for spread films near 0°). These distributions indicate that for these films, crystalline domains are more edge-on (i.e., where the side chain is perpendicular to the substrate) than in spray-coated films. Indeed, spray-coated films had the highest ratio of face-on to edge-on crystallites at ~3. Spin-coated and sheared films had face-on to edge-on ratios of 1.15 and 1.44, respectively, while spread films had the lowest ratio among the four deposition processes (~1.0) (Figure 7d). The high edge-on texturing in spread films has previously been attributed to the migration of low-surface energy side chains to the polymer−air interface during the evaporation process.[47,58] As such, solution spreading with high boiling point solvents thermodynamically favors the formation of edge-on oriented crystallites at the dielectric−polymer interface.[22,23,50,56]

We also quantified the relative proportion of crystalline domains by calculating the relative degree of crystallinity (rDoC) for each film (Figure 7d). These values were then normalized to the calculated crystallinity of spin-coated films, which had the highest degree of crystallinity. Spread and sheared films were almost identical in rDoC, differing by only 5%. Spray-coated films were the least crystalline with a normalized rDoC of ~50%.

Last, we compared the progression of the paracrystalline disorder in crystallites by analyzing the full width at half-maximum (fwhm) and coherence length as determined from the (100) and (200) peaks (Figure 7e−g).[59] For spin, spread, and sheared films, the fwhm of the lamellar peak increased with the diffraction order (m), which is indicative of cumulative disorder in the crystalline domains (Figure 7f). The variations in the fwhm across different deposition processes ultimately influence the coherence length (Figure 7g), which refers to the distance over which long-range order persists in the crystalline domains. The greater coherence length of spread films relative to spin-coated films has previously only been observed for P3HT nanowires,[60] but here, we show that the improvement in long-range order occurs in P3HpT films as well.

Interestingly, our findings suggest that spray-coated films have comparable mobilities to spin-coated films despite a lower proportion of edge-on texturing and rDoC (Figure 7d), as well as a shorter coherence length (Figure 7g). A previous study comparing spun and sprayed films of polythieno[3,4-b]-thiophene-co-benzodithiophene:[6,6]-phenyl-C71-butyric acid methyl ester (PTB7:$PC_{71}BM$) also suggested that spray coating results in a significantly reduced order of molecular packing.[34] Together, our results suggest that the high mobility of spray-coated films likely arises from the presence of the favorable short-range order (as indicated by the high aggregate fraction, Figure 5) rather than the long-range order in crystalline domains. X-ray diffraction measurements also reveal several morphological differences that could contribute to the high mobility of interfacially spread films. First, our calculations of face-on to edge-on population ratios suggest that spread films have the greatest proportion of edge-on texturing (Figure 7d), which agrees with previous studies on interfacial spreading.[22,23,50,56] Edge-on texturing has been shown to be the preferred orientation for good mobility in transistors (though recent studies have shown that crystallite orientation alone does not determine mobility[61,62]).[63,64] Second, spread films have the greatest coherence length (~15% greater than sheared and spin-coated films, Figure 7g), which is also consistent with previous observations.[60] Third, we note that additional GIXD measurements suggest that spread films tend to show more intense scattering intensities along the π-stacking (010) direction, which could also play a role in the higher mobilities (Figure S9). Unfortunately, it is

https://doi.org/10.1021/acsami.1c13043
ACS Appl. Mater. Interfaces XXXX, XXX, XXX−XXX

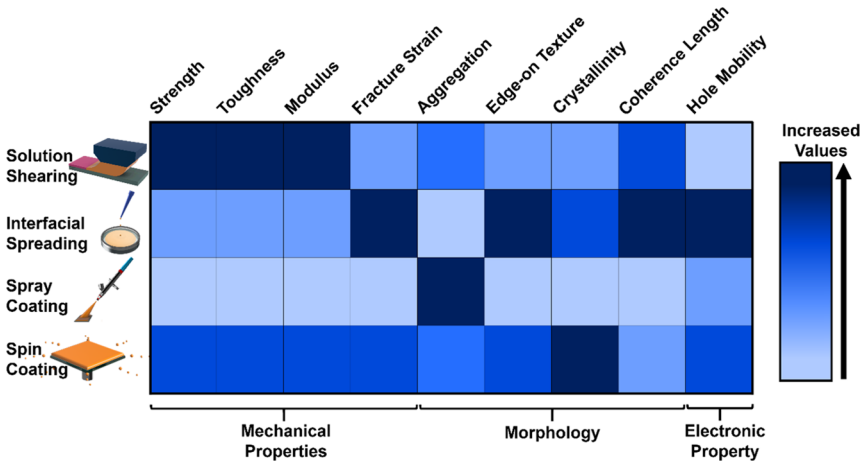

Figure 9. Summary of the findings from this work comparing P3HpT films deposited from four deposition processes.

unclear from our morphological characterization why sheared films have the lowest mobilities despite a relatively large coherence length (Figure 7g), high edge-on texturing, and high rDoC (Figure 7d).

This interrogation of the crystalline morphologies offers an explanation for the improved mobilities of interfacially spread and spray-coated films. However, we find that the mechanical properties of P3HpT films do not seem to be influenced by the crystalline domains of the film. No clear correlation was observed between crystallographic features (i.e., atomic packing distances, relative degree of crystallinity, and coherence length) and the mechanical responses of the films. Previous studies have elucidated the effect of secondary interactions (such as van der Waals forces and π-stacking interactions) on the mechanical properties of a semiconducting film,[7,65−67] suggesting that increased lamellar spacing and $\pi-\pi$ spacing is expected to result in a weaker and less stiff film. Likewise, works from the O'Connor and DeLongchamp laboratories have shown that biaxial strain can be utilized to reorient the texturing of P3HT films (from predominantly edge-on to predominantly face-on),[61,68] thus suggesting that the molecular texture is influenced by strain. (The Gu group has shown a similar result with a donor−acceptor polymer.[69]) Additionally, work by Kim and co-workers has shown that decreasing the crystallinity of P3HT, by decreasing the regioregularity, results in a weaker, less stiff, and more extensible film.[70] However, we observed no correlation between secondary interactions, crystallinity, or paracrystalline disorder and the mechanical responses of the films, perhaps because the proportion of crystalline domains in P3HpT films is too small to influence the mechanical properties. As such, these results reinforce the idea that crystalline domains predominantly dictate the electronic properties of P3HpT films, while the amorphous domains predominantly dictate the mechanical response of P3HpT films. We summarize our morphological characterization in Figure 8.

5. CONCLUSIONS

This study examines how the mechanical properties and charge-transport properties of P3HpT are mediated by morphology, as influenced by the deposition process (Figure 9). When comparing these deposition processes, we draw five significant conclusions. First, interfacially spread P3HpT films have the greatest deformability (among films formed from scalable deposition processes) and the highest mobilities. Thus, for applications requiring mechanical compliance, interfacially spread films thus appear to offer "the best of both worlds". Second, sheared P3HpT films are the most mechanically robust in that they have the highest modulus, strength, and toughness. Thus, solution shearing should be preferred for applications that must withstand mechanical insult. Third, spray-coated films demonstrate very poor mechanical behavior in all respects. However, spray coating is the least expensive process, and it is unique among all studied processes in this work in that it enables patterning through stencil masks. Therefore, further efforts should be made in studying how spray coating can be used in conjunction with semiconducting polymers to obtain films of higher quality. Fourth, we observe that spin coating provides a "middle-of-the-road" for all measurements. Along with its affordability and ease of use, these "representative" measurements make spin coating a powerful tool at the pilot scale. Last, our comparison of P3HpT and P3BT films suggest that effects of the deposition process on the tensile response of the polymer films possibly hold true for both lower-T_g and higher-T_g polymers. Therefore, we find that the deposition process and their processing parameters can have a significant effect on the mechanical properties, electronic properties, and morphology of conjugated polymers.

One limitation of this study is that it used only one set of conditions for each deposition process. In reality, the parameters of each process could be tuned to allow for a semi-infinite set of permutations. While our experimental choices were born out of a desire to obtain a tractable data set (i.e., to characterize films of comparable thicknesses), such decisions have practical and scientific consequences. For example, our GIXD results revealed no correlation between parameters associated with the crystalline regions and the mechanical properties. It is, however, possible that the characteristics of the crystalline phases do indeed affect the mechanical response, but in ways that are counterbalanced by other characteristics considered in this paper—e.g., T_g, free volume, and surface topography. A second potential limitation of this study is the choice of polymer. Although polythiophenes are commonly used as models for other semiconducting polymers, interest in the last decade or so has shifted significantly to donor−acceptor (D−A) polymers.[7] There has been considerable interest in D−A polymers synthesized to have low glass transition temperatures by

https://doi.org/10.1021/acsami.1c13043
ACS Appl. Mater. Interfaces XXXX, XXX, XXX−XXX

means of structural modification (e.g., conjugation break spacers and side chain modifications), blending with elastomers or nonconjugated polymers, or polymerization of block copolymers with nonconjugated segments.[6,15] However, most D−A polymers have high glass transition temperatures and greatly different chemical structures, and the same effects on crystalline morphology have yet to be compared using a high-T_g D−A polymer. Our initial results, however, do suggest that the effects of the deposition process on the mechanical responses of P3HpT and P3BT films are consistent. Considering the scarcity of process-property studies on the mechanical properties of semiconducting polymers, we believe that this study offers a good starting framework for future work in this research area.

■ ASSOCIATED CONTENT

Supporting Information

The Supporting Information is available free of charge at https://pubs.acs.org/doi/10.1021/acsami.1c13043.

Experimental methods, fracture mechanism of spray-coated films, investigation of anisotropy for sheared films, mobility count plots, and additional GIXD measurements (PDF)

Spin coating (MP4)

Interfacial spreading (MP4)

Solution shearing (MP4)

Spray coating (MP4)

■ AUTHOR INFORMATION

Corresponding Author

Darren J. Lipomi − *Department of Nanoengineering and Chemical Engineering Program, University of California, San Diego, La Jolla, California 92093-0448, United States;* orcid.org/0000-0002-5808-7765; Email: dlipomi@eng.ucsd.edu

Authors

Kartik Choudhary − *Department of Nanoengineering and Chemical Engineering Program, University of California, San Diego, La Jolla, California 92093-0448, United States;* orcid.org/0000-0003-2611-8982

Alexander X. Chen − *Department of Nanoengineering and Chemical Engineering Program, University of California, San Diego, La Jolla, California 92093-0448, United States;* orcid.org/0000-0003-1919-6755

Gregory M. Pitch − *Department of Chemistry and Biochemistry, University of California, Santa Cruz, Santa Cruz, California 95064, United States*

Rory Runser − *Department of Nanoengineering and Chemical Engineering Program, University of California, San Diego, La Jolla, California 92093-0448, United States*

Armando Urbina − *Department of Nanoengineering and Chemical Engineering Program, University of California, San Diego, La Jolla, California 92093-0448, United States*

Tim J. Dunn − *Stanford Synchrotron Radiation Light Source, SLAC National Accelerator Laboratory, Menlo Park, California 94025, United States*

Moses Kodur − *Department of Nanoengineering and Chemical Engineering Program, University of California, San Diego, La Jolla, California 92093-0448, United States;* orcid.org/0000-0002-3890-2945

Andrew T. Kleinschmidt − *Department of Nanoengineering and Chemical Engineering Program, University of California, San Diego, La Jolla, California 92093-0448, United States;* orcid.org/0000-0002-6036-6878

Benjamin G. Wang − *Department of Nanoengineering and Chemical Engineering Program, University of California, San Diego, La Jolla, California 92093-0448, United States*

Jordan A. Bunch − *Department of Nanoengineering and Chemical Engineering Program, University of California, San Diego, La Jolla, California 92093-0448, United States*

David P. Fenning − *Department of Nanoengineering and Chemical Engineering Program, University of California, San Diego, La Jolla, California 92093-0448, United States;* orcid.org/0000-0002-4609-9312

Alexander L. Ayzner − *Department of Chemistry and Biochemistry, University of California, Santa Cruz, Santa Cruz, California 95064, United States;* orcid.org/0000-0002-6549-4721

Complete contact information is available at: https://pubs.acs.org/10.1021/acsami.1c13043

Author Contributions

‖K.C. and A.X.C. contributed equally.

Notes

The authors declare no competing financial interest.

■ ACKNOWLEDGMENTS

This work was supported by the Air Force Office of Scientific Research (AFOSR) grant no. FA9550-19-1-0278. K.C. acknowledges additional support as a Hellman Scholar and an Intel Scholar provided through the Academic Enrichment Program (AEP) at UCSD through the following awards: The Undergraduate Research Scholarship and Semiconductor Research Corporation Scholarship. In addition, R.R. received support from the National Science Foundation Graduate Research Fellowship (NSF GRFP) under grant no. DGE-1144086. D.P.F. acknowledges financial support from the California Energy Commission (EPC-19-004). A.L.A. acknowledges financial support from the National Science Foundation under grant no. 1848069. This work was performed in part at the San Diego Nanotechnology Infrastructure (SDNI) of UC San Diego, a member of the National Nanotechnology Coordinated Infrastructure, which is supported by the National Science Foundation (Grant ECCS-1542148). Use of the Stanford Synchrotron Radiation Light Source, SLAC National Accelerator Laboratory, is supported by the U.S. Department of Energy, Office of Science, and Office of Basic Energy Sciences under Contract DEAC02-76SF00515. The authors would also like to thank Julian Ramirez, Mickey Finn, and Guillermo Esparza for insightful discussions.

■ REFERENCES

(1) Amb, C. M.; Dyer, A. L.; Reynolds, J. R. Navigating the Color Palette of Solution-Processable Electrochromic Polymers. *Chem. Mater.* **2010**, *23*, 397−415.

(2) Inal, S.; Rivnay, J.; Suiu, A.-O.; Malliaras, G. G.; McCulloch, I. Conjugated Polymers in Bioelectronics. *Acc. Chem. Res.* **2018**, *51*, 1368−1376.

(3) Facchetti, A. π-Conjugated Polymers for Organic Electronics and Photovoltaic Cell Applications. *Chem. Mater.* **2010**, *23*, 733−758.

(4) Awartani, O.; Lemanski, B. I.; Ro, H. W.; Richter, L. J.; DeLongchamp, D. M.; O'Connor, B. T. Correlating Stiffness,

Ductility, and Morphology of Polymer:Fullerene Films for Solar Cell Applications. *Adv. Energy Mater.* **2013**, *3*, 399−406.
(5) Zhang, S.; Ocheje, M. U.; Luo, S.; Ehlenberg, D.; Appleby, B.; Weller, D.; Zhou, D.; Rondeau-Gagné, S.; Gu, X. Probing the Viscoelastic Property of Pseudo Free-Standing Conjugated Polymeric Thin Films. *Macromol. Rapid Commun.* **2018**, *39*, 1800092.
(6) Chen, A. X.; Kleinschmidt, A. T.; Choudhary, K.; Lipomi, D. J. Beyond Stretchability: Strength, Toughness, and Elastic Range in Semiconducting Polymers. *Chem. Mater.* **2020**, *32*, 7582−7601.
(7) Root, S. E.; Savagatrup, S.; Printz, A. D.; Rodriquez, D.; Lipomi, D. J. Mechanical Properties of Organic Semiconductors for Stretchable, Highly Flexible, and Mechanically Robust Electronics. *Chem. Rev.* **2017**, *117*, 6467−6499.
(8) Diao, Y.; Shaw, L.; Bao, Z.; Mannsfeld, S. C. B. Morphology Control Strategies for Solution-Processed Organic Semiconductor Thin Films. *Energy Environ. Sci.* **2014**, *7*, 2145−2159.
(9) Fenner, R. T. Processing Properties of Polymers*Princ. Polym. Process, 1st Edition.* Palgrave: London, 1979, 16−32.
(10) Li, Y.; Sun, H.; Shi, Y.; Tsukagoshi, K. Patterning Technology for Solution-Processed Organic Crystal Field-Effect Transistors. *Sci. Technol. Adv. Mater.* **2014**, *15*, 024203.
(11) Beaujuge, P. M.; Reynolds, J. R. Color Control in π-Conjugated Organic Polymers for Use in Electrochromic Devices. *Chem. Rev.* **2010**, *110*, 268−320.
(12) Søndergaard, R.; Hösel, M.; Angmo, D.; Larsen-Olsen, T. T.; Krebs, F. C. Roll-to-Roll Fabrication of Polymer Solar Cells. *Mater. Today* **2012**, *15*, 36−49.
(13) Whitesides, G. M. Physical-Organic Chemistry: A Swiss Army Knife. *Isr. J. Chem.* **2016**, *56*, 66−82.
(14) Qian, Z.; Cao, Z.; Galuska, L.; Zhang, S.; Xu, J.; Gu, X. Glass Transition Phenomenon for Conjugated Polymers. *Macromol. Chem. Phys.* **2019**, *220*, 1900062.
(15) Higashihara, T. Strategic design and synthesis of π-conjugated polymers suitable as intrinsically stretchable semiconducting materials. *Polym. J.* **2021**, *53*, 1061−1071.
(16) Balar, N.; Xiong, Y.; Ye, L.; Li, S.; Nevola, D.; Dougherty, D. B.; Hou, J.; Ade, H.; O'Connor, B. T. Role of Polymer Segregation on the Mechanical Behavior of All-Polymer Solar Cell Active Layers. *ACS Appl. Mater. Interfaces* **2017**, *9*, 43886−43892.
(17) Wang, Y.; Zhu, Q.; Naveed, H. B.; Zhao, H.; Zhou, K.; Ma, W. Sequential Blade-Coated Acceptor and Donor Enables Simultaneous Enhancement of Efficiency, Stability, and Mechanical Properties for Organic Solar Cells. *Adv. Energy Mater.* **2020**, *10*, 1903609.
(18) Lin, B.; Zhang, L.; Zhao, H.; Xu, X.; Zhou, K.; Zhang, S.; Gou, L.; Fan, B.; Zhang, L.; Yan, H.; Gu, X.; Ying, L.; Huang, F.; Cao, Y.; Ma, W. Molecular Packing Control Enables Excellent Performance and Mechanical Property of Blade-Cast All-Polymer Solar Cells. *Nano Energy* **2019**, *59*, 277−284.
(19) Spano, F. C.; Silva, C. H- and J-Aggregate Behavior in Polymeric Semiconductors. *Annu. Rev. Phys. Chem.* **2014**, *65*, 477−500.
(20) Root, S. E.; Jackson, N. E.; Savagatrup, S.; Arya, G.; Lipomi, D. J. Modelling the Morphology and Thermomechanical Behaviour of Low-Bandgap Conjugated Polymers and Bulk Heterojunction Films. *Energy Environ. Sci.* **2017**, *10*, 558−569.
(21) Helgesen, M.; Søndergaard, R.; Krebs, F. C. Advanced Materials and Processes for Polymer Solar Cell Devices. *J. Mater. Chem.* **2009**, *20*, 36−60.
(22) Morita, T.; Singh, V.; Nagamatsu, S.; Oku, S.; Takashima, W.; Kaneto, K. Enhancement of Transport Characteristics in Poly(3-Hexylthiophene) Films Deposited with Floating Film Transfer Method. *Appl. Phys. Express* **2009**, *2*, 111502.
(23) Choi, G.; Lee, K.; Oh, S.; Seo, J.; Kim, C.; An, T. K.; Lee, J.; Lee, H. S. Understanding Marangoni Flow-Driven Solidification of Polymer Semiconducting Films on an Aqueous Substrate. *J. Mater. Chem. C* **2020**, *8*, 10010−10020.
(24) Sung, Y.; Shin, E.-Y.; Noh, Y.-Y.; Lee, J.-Y. Flexible Bottom-Gated Organic Field-Effect Transistors Utilizing Stamped Polymer Layers from the Surface of Water. *ACS Appl. Mater. Interfaces* **2020**, *12*, 25092−25099.
(25) Esparza, G. L.; Lipomi, D. J. Solid-Phase Deposition: Conformal Coverage of Micron-Scale Relief Structures with Stretchable Semiconducting Polymers. *ACS Mater. Lett.* **2021**, *3*, 988−995.
(26) Runser, R.; Root, S. E.; Ober, D. E.; Choudhary, K.; Chen, A. X.; Dhong, C.; Urbina, A. D.; Lipomi, D. J. Interfacial Drawing: Roll-to-Roll Coating of Semiconducting Polymer and Barrier Films onto Plastic Foils and Textiles. *Chem. Mater.* **2019**, *31*, 9078−9086.
(27) Noh, J.; Jeong, S.; Lee, J.-Y. Ultrafast Formation of Air-Processable and High-Quality Polymer Films on an Aqueous Substrate. *Nat. Commun.* **2016**, *7*, 12374.
(28) Pandey, M.; Sadakata, S.; Nagamatsu, S.; Pandey, S. S.; Hayase, S.; Takashima, W. Layer-by-Layer Coating of Oriented Conjugated Polymer Films towards Anisotropic Electronics. *Synth. Met.* **2017**, *227*, 29−36.
(29) Nawaz, A.; Tavares, A. C. B.; Trang Do, T.; Patil, B. B.; Sonar, P.; Hümmelgen, I. A. Experimental and Modeling Study of Low-Voltage Field-Effect Transistors Fabricated with Molecularly Aligned Copolymer Floating Films. *Flexible Printed Electron.* **2018**, *3*, 015006.
(30) Shaw, L.; Hayoz, P.; Diao, Y.; Reinspach, J. A.; To, J. W. F.; Toney, M. F.; Weitz, R. T.; Bao, Z. Direct Uniaxial Alignment of a Donor-Acceptor Semiconducting Polymer Using Single-Step Solution Shearing. *ACS Appl. Mater. Interfaces* **2016**, *8*, 9285−9296.
(31) Smilgies, D.-M.; Li, R.; Giri, G.; Chou, K. W.; Diao, Y.; Bao, Z.; Amassian, A. Look Fast: Crystallization of Conjugated Molecules during Solution Shearing Probed in-Situ and in Real Time by X-Ray Scattering. *Phys. Status Solidi RRL* **2013**, *7*, 177−179.
(32) Giri, G.; DeLongchamp, D. M.; Reinspach, J.; Fischer, D. A.; Richter, L. J.; Xu, J.; Benight, S.; Ayzner, A.; He, M.; Fang, L.; Xue, G.; Toney, M. F.; Bao, Z. Effect of Solution Shearing Method on Packing and Disorder of Organic Semiconductor Polymers. *Chem. Mater.* **2015**, *27*, 2350−2359.
(33) Giri, G.; Verploegen, E.; Mannsfeld, S. C. B.; Atahan-Evrenk, S.; Kim, D. H.; Lee, S. Y.; Becerril, H. A.; Aspuru-Guzik, A.; Toney, M. F.; Bao, Z. Tuning Charge Transport in Solution-Sheared Organic Semiconductors Using Lattice Strain. *Nature* **2011**, *480*, 504−508.
(34) Al-Hussein, M.; Herzig, E. M.; Schindler, M.; Löhrer, F.; Palumbiny, C. M.; Wang, W.; Roth, S. V.; Müller-Buschbaum, P. Comparative Study of the Nanomorphology of Spray and Spin Coated PTB7 Polymer: Fullerene Films. *Polym. Eng. Sci.* **2016**, *56*, 889−894.
(35) Noebels, M.; Cross, R. E.; Evans, D. A.; Finlayson, C. E. Characterization of Spray-Coating Methods for Conjugated Polymer Blend Thin Films. *J. Mater. Sci.* **2014**, *49*, 4279−4287.
(36) Bielecka, U.; Lutsyk, P.; Janus, K.; Sworakowski, J.; Bartkowiak, W. Effect of Solution Aging on Morphology and Electrical Characteristics of Regioregular P3HT FETs Fabricated by Spin Coating and Spray Coating. *Org. Electron.* **2011**, *12*, 1768−1776.
(37) Khim, D.; Baeg, K.-J.; Yu, B.-K.; Kang, S.-J.; Kang, M.; Chen, Z.; Facchetti, A.; Kim, D.-Y.; Noh, Y.-Y. Spray-Printed Organic Field-Effect Transistors and Complementary Inverters. *J. Mater. Chem. C* **2013**, *1*, 1500−1506.
(38) Scarratt, N. W.; Griffin, J.; Wang, T.; Zhang, Y.; Yi, H.; Iraqi, A.; Lidzey, D. G. Polymer-Based Solar Cells Having an Active Area of 1.6 Cm2 Fabricated via Spray Coating. *APL Mater.* **2015**, *3*, 126108.
(39) Savagatrup, S.; Printz, A. D.; Wu, H.; Rajan, K. M.; Sawyer, E. J.; Zaretski, A. V.; Bettinger, C. J.; Lipomi, D. J. Viability of Stretchable Poly(3-Heptylthiophene) (P3HpT) for Organic Solar Cells and Field-Effect Transistors. *Synth. Met.* **2015**, *203*, 208−214.
(40) Savikhin, V.; Jagadamma, L. K.; Purvis, L. J.; Robertson, I.; Oosterhout, S. D.; Douglas, C. J.; Samuel, I. D. W.; Toney, M. F. Morphological, Chemical, and Electronic Changes of the Conjugated Polymer PTB7 with Thermal Annealing. *iScience* **2018**, *2*, 182−192.
(41) Selivanova, M.; Zhang, S.; Billet, B.; Malik, A.; Prine, N.; Landry, E.; Gu, X.; Xiang, P.; Rondeau-Gagné, S. Branched Polyethylene as a Plasticizing Additive to Modulate the Mechanical

https://doi.org/10.1021/acsami.1c13043
ACS Appl. Mater. Interfaces XXXX, XXX, XXX−XXX

Properties of π-Conjugated Polymers. *Macromolecules* **2019**, *52*, 7870−7877.
(42) Kim, J.-H.; Nizami, A.; Hwangbo, Y.; Jang, B.; Lee, H.-J.; Woo, C.-S.; Hyun, S.; Kim, T.-S. Tensile Testing of Ultra-Thin Films on Water Surface. *Nat. Commun.* **2013**, *4*, 1−6.
(43) Wang, S.; Fabiano, S.; Himmelberger, S.; Puzinas, S.; Crispin, X.; Salleo, A.; Berggren, M. Experimental Evidence That Short-Range Intermolecular Aggregation Is Sufficient for Efficient Charge Transport in Conjugated Polymers. *Proc. Natl. Acad. Sci. U.S.A.* **2015**, *112*, 10599−10604.
(44) Root, S. E.; Alkhadra, M. A.; Rodriquez, D.; Printz, A. D.; Lipomi, D. J. Measuring the Glass Transition Temperature of Conjugated Polymer Films with Ultraviolet-Visible Spectroscopy. *Chem. Mater.* **2017**, *29*, 2646−2654.
(45) Xie, R.; Weisen, A. R.; Lee, Y.; Aplan, M. A.; Fenton, A. M.; Masucci, A. E.; Kempe, F.; Sommer, M.; Pester, C. W.; Colby, R. H.; Gomez, E. D. Glass Transition Temperature from the Chemical Structure of Conjugated Polymers. *Nat. Commun.* **2020**, *11*, 1−8.
(46) Ito, Y.; Virkar, A. A.; Mannsfeld, S.; Oh, J. H.; Toney, M.; Locklin, J.; Bao, Z. Crystalline Ultrasmooth Self-Assembled Monolayers of Alkylsilanes for Organic Field-Effect Transistors. *J. Am. Chem. Soc.* **2009**, *131*, 9396−9404.
(47) Wei, Q.; Miyanishi, S.; Tajima, K.; Hashimoto, K. Enhanced Charge Transport in Polymer Thin-Film Transistors Prepared by Contact Film Transfer Method. *ACS Appl. Mater. Interfaces* **2009**, *1*, 2660−2666.
(48) Lee, J.-H.; Chung, J. Y.; Stafford, C. M. Effect of Confinement on Stiffness and Fracture of Thin Amorphous Polymer Films. *ACS Macro Lett.* **2011**, *1*, 122−126.
(49) Moulton, J.; Smith, P. Electrical and Mechanical Properties of Oriented Poly(3-Alkylthiophenes): 2. Effect of Side-Chain Length. *Polymer* **1992**, *33*, 2340−2347.
(50) Pandey, M.; Kumari, N.; Nagamatsu, S.; Pandey, S. S. Recent Advances in the Orientation of Conjugated Polymers for Organic Field-Effect Transistors. *J. Mater. Chem. C* **2019**, *7*, 13323−13351.
(51) Yang, Y.; Liu, Z.; Chen, J.; Cai, Z.; Wang, Z.; Chen, W.; Zhang, G.; Zhang, X.; Chi, L.; Zhang, D. A Facile Approach to Improve Interchain Packing Order and Charge Mobilities by Self-Assembly of Conjugated Polymers on Water. *Adv. Sci.* **2018**, *5*, 1801497.
(52) O'Connor, B.; Chan, E. P.; Chan, C.; Conrad, B. R.; Richter, L. J.; Kline, R. J.; Heeney, M.; McCulloch, I.; Soles, C. L.; DeLongchamp, D. M. Correlations between Mechanical and Electrical Properties of Polythiophenes. *ACS Nano* **2010**, *4*, 7538−7544.
(53) Printz, A. D.; Lipomi, D. J. Competition between Deformability and Charge Transport in Semiconducting Polymers for Flexible and Stretchable Electronics. *Appl. Phys. Rev.* **2016**, *3*, 021302.
(54) Zheng, Y.; Wang, G. J. N.; Kang, J.; Nikolka, M.; Wu, H. C.; Tran, H.; Zhang, S.; Yan, H.; Chen, H.; Yuen, P. Y.; Mun, J.; Dauskardt, R. H.; McCulloch, I.; Tok, J. B. H.; Gu, X.; Bao, Z. An Intrinsically Stretchable High-Performance Polymer Semiconductor with Low Crystallinity. *Adv. Funct. Mater.* **2019**, *29*, 1905340.
(55) Ding, Z.; Liu, D.; Zhao, K.; Han, Y. Optimizing Morphology to Trade Off Charge Transport and Mechanical Properties of Stretchable Conjugated Polymer Films. *Macromolecules* **2021**, *54*, 3907−3926.
(56) Pandey, M.; Gowda, A.; Nagamatsu, S.; Kumar, S.; Takashima, W.; Hayase, S.; Pandey, S. S. Rapid Formation and Macroscopic Self-Assembly of Liquid-Crystalline, High-Mobility, Semiconducting Thienothiophene. *Adv. Mater. Interfaces* **2018**, *5*, 1700875.
(57) Osaka, I.; Takimiya, K. Backbone Orientation in Semiconducting Polymers. *Polymer* **2015**, *59*, A1−A15.
(58) Hao, X. T.; Hosokai, T.; Mitsuo, N.; Kera, S.; Okudaira, K. K.; Mase, K.; Ueno, N. Control of the Interchain π−π Interaction and Electron Density Distribution at the Surface of Conjugated Poly(3-hexylthiophene) Thin Films. *J. Phys. Chem. B* **2007**, *111*, 10365−10372.
(59) Rivnay, J.; Mannsfeld, S. C. B.; Miller, C. E.; Salleo, A.; Toney, M. F. Quantitative Determination of Organic Semiconductor Microstructure from the Molecular to Device Scale. *Chem. Rev.* **2012**, *112*, 5488−5519.
(60) Kim, Y.-J.; Jung, H.-T.; Ahn, C. W.; Jeon, H.-J. Simultaneously Induced Self-Assembly of Poly(3-Hexylthiophene) (P3HT) Nanowires and Thin-Film Fabrication via Solution-Floating Method on a Water Substrate. *Adv. Mater. Interfaces* **2017**, *4*, 1700342.
(61) Gargi, D.; Kline, R. J.; DeLongchamp, D. M.; Fischer, D. A.; Toney, M. F.; O'Connor, B. T. Charge Transport in Highly Face-On Poly(3-Hexylthiophene) Films. *J. Phys. Chem. C* **2013**, *117*, 17421−17428.
(62) Rivnay, J.; Toney, M. F.; Zheng, Y.; Kauvar, I. V.; Chen, Z.; Wagner, V.; Facchetti, A.; Salleo, A. Unconventional Face-On Texture and Exceptional In-Plane Order of a High Mobility n-Type Polymer. *Adv. Mater.* **2010**, *22*, 4359−4363.
(63) Schuettfort, T.; Thomsen, L.; McNeill, C. R. Observation of a Distinct Surface Molecular Orientation in Films of a High Mobility Conjugated Polymer. *J. Am. Chem. Soc.* **2013**, *135*, 1092−1101.
(64) Kim, G.; Kang, S.-J.; Dutta, G. K.; Han, Y.-K.; Shin, T. J.; Noh, Y.-Y.; Yang, C. A Thienoisoindigo-Naphthalene Polymer with Ultrahigh Mobility of 14.4 cm2/V·s That Substantially Exceeds Benchmark Values for Amorphous Silicon Semiconductors. *J. Am. Chem. Soc.* **2014**, *136*, 9477−9483.
(65) Li, Y.; Tatum, W. K.; Onorato, J. W.; Zhang, Y.; Luscombe, C. K. Low Elastic Modulus and High Charge Mobility of Low-Crystallinity Indacenodithiophene-Based Semiconducting Polymers for Potential Applications in Stretchable Electronics. *Macromolecules* **2018**, *51*, 6352−6358.
(66) Postema, A. R.; Liou, K.; Wudl, F.; Smith, P. Highly Oriented Low-Modulus Materials from Liquid-Crystalline Polymers: The Ultimate Penalty for Solubilizing Alkyl Side Chains. *Macromolecules* **2002**, *23*, 1842−1845.
(67) Sommerville, P. J. W.; Li, Y.; Dong, B. X.; Zhang, Y.; Onorato, J. W.; Tatum, W. K.; Balzer, A. H.; Stingelin, N.; Patel, S. N.; Nealey, P. F.; Luscombe, C. K. Elucidating the Influence of Side-Chain Circular Distribution on the Crack Onset Strain and Hole Mobility of Near-Amorphous Indacenodithiophene Copolymers. *Macromolecules* **2020**, *53*, 7511−7518.
(68) O'Connor, B.; Kline, R. J.; Conrad, B. R.; Richter, L. J.; Gundlach, D.; Toney, M. F.; DeLongchamp, D. M. Anisotropic Structure and Charge Transport in Highly Strain-Aligned Regioregular Poly(3-Hexylthiophene). *Adv. Funct. Mater.* **2011**, *21*, 3697−3705.
(69) Zhang, S.; Alesadi, A.; Mason, G. T.; Chen, K. L.; Freychet, G.; Galuska, L.; Cheng, Y. H.; St. Onge, P. B. J.; Ocheje, M. U.; Ma, G.; Qian, Z.; Dhakal, S.; Ahmad, Z.; Wang, C.; Chiu, Y. C.; Rondeau-Gagné, S.; Xia, W.; Gu, X. Molecular Origin of Strain-Induced Chain Alignment in PDPP-Based Semiconducting Polymeric Thin Films. *Adv. Funct. Mater.* **2021**, *31*, 2100161.
(70) Kim, J.-S.; Kim, J.-H.; Lee, W.; Yu, H.; Kim, H. J.; Song, I.; Shin, M.; Oh, J. H.; Jeong, U.; Kim, T.-S.; Kim, B. J. Tuning Mechanical and Optoelectrical Properties of Poly(3-Hexylthiophene) through Systematic Regioregularity Control. *Macromolecules* **2015**, *48*, 4339−4346.

https://doi.org/10.1021/acsami.1c13043
ACS Appl. Mater. Interfaces XXXX, XXX, XXX−XXX